High Power Dielectric Reflectarray Antenna using 3D Printing Technology

Binke Huang [1], Qiwen Qiang [1], and Guy A. E. Vandenbosch [2]

[1] Department of Information and Telecommunication Engineering
Xi'an Jiaotong University, Xi'an 710049, China
bkhuang@mail.xjtu.edu.cn, foreverfree2@sina.com

[2] Department of Electrical Engineering, Division ESAT-TELEMIC
KU Leuven, B-3001 Leuven, Belgium
guy.vandenbosch@esat.kuleuven.be

Abstract ─ A high power dielectric reflectarray with a continuous variation of the effective permittivity of a dielectric slab is proposed, based on a cross-shaped element implemented in the slab. The improved method used to retrieve the effective permittivity from the S parameters shows that a continuously changing effective relative permittivity from 1.25 to 3.4 can be reached by adjusting the notch width of the cross-shape, yielding a full 360° range of phase shifts at 9.3GHz. An array of 10×10 elements is designed to verify the radiation properties.Simulation results show that a main beam direction of 25° and a maximum gain of 19.5dB can be realized at the 9.3GHz center frequency. The power capacity of the element reaches 371kW, opening the possibility of high power applications. Fused Deposition Modelling (FDM), a specific approach in 3D printing, was employed for the fabrication of a prototype. This technology significantly reduces material cost and manufacturing time.

Index Terms ─ Dielectric reflectarray, Fused Deposition Modeling (FDM), high power.

I. INTRODUCTION

The reflectarray antenna is regarded as a good alternative for traditional parabolic antennas and array antennas because of its low profile, high gain, beam steering possibilities and simple horn feeding [1-2]. A reflectarray can be achieved by dividing the reflector surface into a sub-wavelength grid of individual metamaterial unit cells, each with a variable reflection phase. However, since periodic unit cells may exhibit dielectric breakdown at high powers [3], which would change the radiation properties of the antenna and introduce irreversible damage, care must be taken so that neither dielectric nor air breakdown occurs under operating conditions.

In recent years, in order to improve the mobility of high power parabolic antennas equipped on vehicles, the reflectarray is considered as a promising alternative to the bulky conventional parabolic antenna in many high power applications. In 2015, Zhao *et al.* proposed an element of double square rings covered with a PTFE layer for an X-band high power reflectarray antenna [4]. In 2017, Gregory *et al.* proposed a shorted circular element unit cell for implementing steerable high power reflectarray [5]. In 2018, Gregory *et al.* proposed metamaterial-based unit cells usable in reflectarrays. They are comprised of end-loaded dipoles with capacitive lumped elements, round edges, and approximate high voltage capacitors as loads to mitigate field enhancement [6-7]. However, all these designs are complex in processing and the power capacity is unable to reach the GW/m^2 regime.

In this paper, we present a kind of dielectric reflectarray element that is feasible to be fabricated by FDM 3D printing technology to replace the traditional microstrip element for power capacity enhancement. The element is composed of a conductive ground and a dielectric block of changing effective permittivity to regulate the reflection phase. An improved method is used to retrieve the effective permittivity of the cross-shaped element based metamaterial slab with periodic boundary from its S parameters. By varying the notch width of the slab, a continuous effective relative permittivity is successfully achieved. This variation in the relative permittivity is used to obtain the required reflection phase shifts in the reflectarray. The power capacity is investigated. A complete reflectarray antenna with 10×10 elements is designed with the full-wave simulation software CST Microwave Studio® [8] to validate the radiation properties, and a 10×10 array is prototyped with 3D printing technology.

II. ELEMENT DESIGN

A. Homogeneous slab of dielectric

Consider a homogeneous dielectric slab backed by a conductive ground. The thickness of the slab is *h*, its

Submitted On: January 24, 2019
Accepted On: April 6, 2019

permittivity is ε, and its loss tangent is tanδ. Assume a normally incident plane wave. Fig. 1 shows the phase and the magnitude of the reflection coefficient versus the relative permittivity of the slab for the case h=25 mm (0.775λ for f=9.3GHz), ε_r=1.0 to 3.5, and tanδ=5.1×10-3 at f=9.1GHz, 9.3GHz and 9.5GHz. The dielectric is inspired by [9] and the height is considerable in order to get sufficient phase shift. It can be seen that when the bulk relative permittivity changes from 1.0 to 3.5, the reflection phase shifts indicate a range of more than 360°. The reflection phase curves are quasi-parallel for the three frequencies. The reflection magnitude varies in between -0.20 and -0.60 dB.

B. The cross-shaped block

Replace the continuous slab by an array of cross-shaped dielectric blocks, as depicted in Fig. 2. The bulk relative permittivity of the dielectric is 3.4. The element spacing is P=16 mm (0.5 λ) to avoid grating lobes. The dimensions of the cross-shaped dielectric blocks are listed in Table 1.

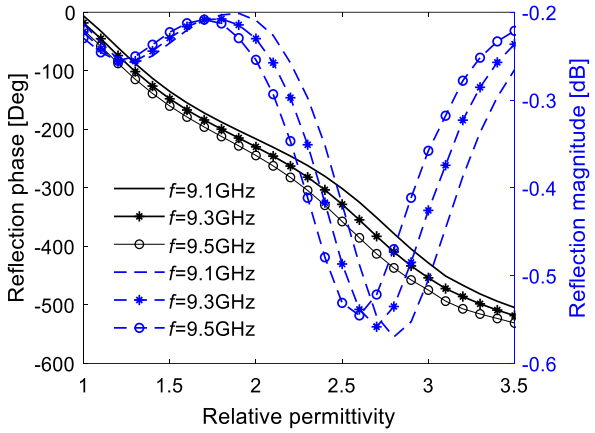

Fig. 1. Reflection coefficient versus relative permittivity of the slab.

Characterizing this block array as an effective homogeneous dielectric slab, we need to remove the ground and retrieve the effective permittivity and permeability from the reflection (S_{11}) and transmission (S_{21}) coefficients for a normally incident plane wave. The S parameters are related to the refractive index n of this effective slab and the free space wave impedance Z by [10]:

$$n = \{\arccos[(1-S_{11}^2+S_{21}^2)/(2S_{21})]\}/(k_0 h), \quad (1)$$

$$Z = \sqrt{[(1+S_{11})^2-S_{21}^2]/[(1-S_{11})^2-S_{21}^2]}, \quad (2)$$

where k_0 denotes the wave number. The permittivity ε and permeability μ are then directly calculated from ε=nZ and μ=n/Z. Figure 3 shows that for the example considered with h=2 mm the retrieved effective permittivity varies with the size of the corner notch w. We can see that an effective relative permittivity from 1.25 to 3.4 can be achieved by properly choosing w. Moreover, the effective relative permittivity is quite stable with a maximum variation of no more than 0.2 for the three different frequencies depicted. This guarantees the desired phase shifts in the frequency band of interest.

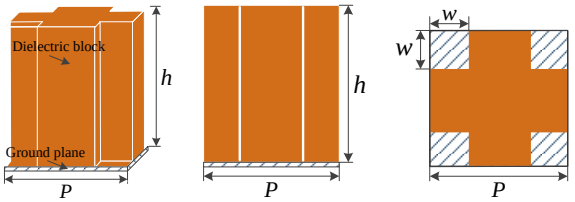

Fig. 2. Element structure with cross-shaped dielectric block: (a) perspective view, (b) front view, and (c) top view.

Table 1: Parameters of cross-shaped dielectric block

Name	Description	Value
H	Height of slab	2 mm
P	Element spacing	16 mm
w	Size of notch	0.5~7.5 mm
ε_r	Effective relative permittivity	3.4
tanδ	Loss tangent	5.1×10^{-3}

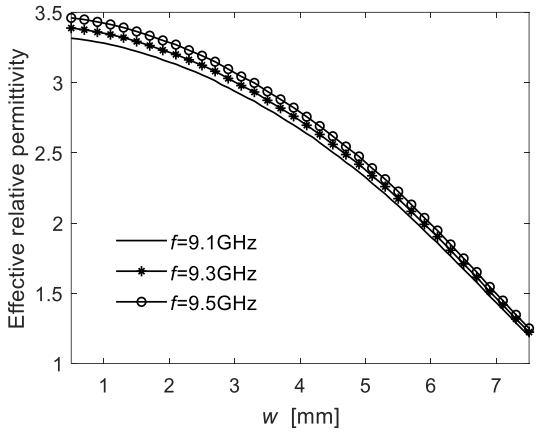

Fig. 3. Retrieved effective relative permittivity versus notch size w, all for h =2 mm.

The height of the cross-shaped block h=2 mm is adopted for achieving a high accuracy when retrieving its effective permittivity from (1). Now the thickness is increased to the original 25 mm, the ground is added again, and the resulting topology is simulated using Ansys HFSS™ with periodic boundaries [11]. Figure 4 shows the resulting phase and magnitude of the reflection coefficient versus the notch size w for normal incidence at f=9.1 GHz, 9.3 GHz and 9.5 GHz. It can be seen that the reflection phase possesses a good linearity and a

similar flatness as for the original homogeneous slab (See Fig. 1). The phase shift is smooth and the ranges for the three different frequencies are all more than 360°. The reflection magnitude for the different frequencies and notch sizes *w* is better than -0.55 dB (0.94), indicating a fairly efficient reflector performance.

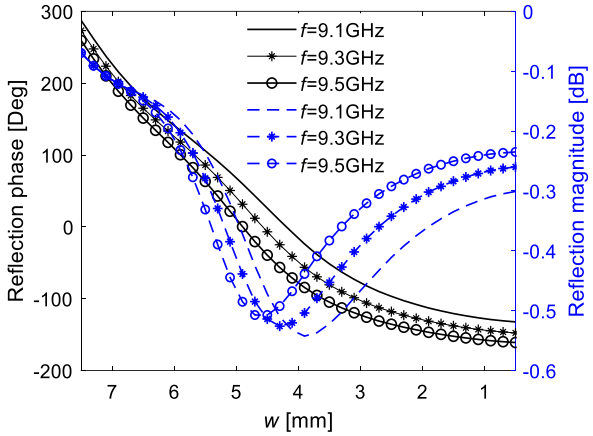

Fig. 4. Reflection coefficient versus notch size *w* simulated with HFSS.

III. REFLECTARRAY DESIGN

A complete dielectric reflectarray antenna is designed in this section. The idea is to generate a transversally changing permittivity by changing the size of the corner notch *w* from block to block and this in such a way that it yields the correct transversally changing reflection phase needed in the reflectarray. The required phase shift for each element (*m*,*n*) located at (x_m, y_n, 0) can be calculated as follows [1]:

$$k_0(r_{mn} - \bar{R}_{mn} \cdot \hat{r}_b) - \Delta\Phi_{mn} = 2\pi N, \quad (3)$$

$$r_{mn} = \sqrt{(x_F - x_m)^2 + (y_F - y_n)^2 + z_F^2}, \quad (4)$$

where k_0 denotes the wave number, $\bar{r}_{mn}$ is the position vector of the mn^{th} element relative to the feed point at (x_F, y_F, z_F) = (0, 0, z_F). $\bar{R}_{mn}$ is the position vector of mn^{th} element relative to (0, 0, 0), $\hat{r}_b$ is the direction vector of the desired pencil beam with (θ_b, φ_b) in a spherical coordinate system, N=1, 2, 3, …, and $\Delta\Phi_{mn}$ is the phase shift introduced by the element of the reflectarray in the reflected wave relative to the incident wave.

The reflectarray topology is illustrated in Fig. 5. The resulting design is an array of 10×10 element blocks with an aperture size of 160mm×160mm, operating at 9.3GHz and fed by a centered pyramid horn. It's phase center is located at a distance F=100 mm from the reflectarray. The desired main beam direction (θ_b, φ_b) is set as (25°, 0°). F corresponds to the focal length of the reflectarray. It is calculated as:

$$F = D/(2\tan\theta_e), \quad (5)$$

where D is the size of the reflector aperture, and θ_e is half the beamwidth where the gain of the feed horn drops by less than 10 dB compared to the broadside maximum. A pyramidal horn antenna with a θ_e of 38° and a standard waveguide WR90 as feeding port was selected [11].

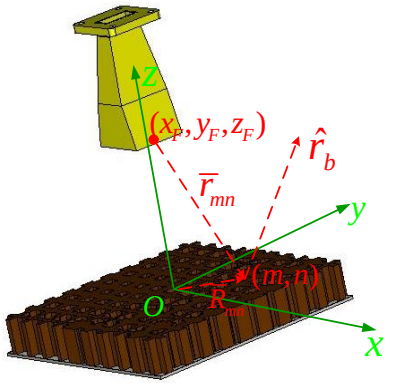

Fig. 5. The designed complete reflectarray.

The simulated radiation pattern in *x*-*z* plane for co-polarization (φ=0°) and in *y*-*z* plane for cross-polarization (φ=90°) at f = 9.3GHz are shown in Fig. 6. The reflected pencil beam is observed at 25 degrees, the maximum gain is 19.5dBi, and the 3dB beamwidth is 14°. The sidelobes are more than 10.5dB lower than the main lobe and the cross-polarization level is 18.2dB below the co-polarization level.

IV. POWER CAPACITY ANALYSIS

The limiting factor in power peak handling is the breakdown strength of the air around the cross-shaped block, which is approximately 3MV/m [7]. This is because, usually, the high power pulse is modulated with a sinusoidal signal and the duty cycle is sufficiently low so that thermal effects can be ignored. The key idea is thus to make a design with a low peak value of the electric field around the element, for a fixed input power. It is obvious that the variation of the notch size *w* leads to a variation of the *E*-field strength distribution. Simulations show that the maximum field distribution for the element occurs at resonance with the reflection phase equaling zero, since the reflected wave and the incident wave are in phase addition. This is for a normally incident plane wave from the positive *z*-direction. In our design this means for w = 4 mm at 9.3 GHz. For a feeding power density p_{in} of the structure of 1W/(0.016m)^2=3.906kW/m^2, the maximum *E*-field strength is 4926 V/m. Figure 7 shows how the maximum absolute value of the total *E*-field varies with the notch size *w* at 9.3 GHz. The maximum power density of the exciting plane wave can be calculated as follows [4]:

$$p_{\max} = [E_b / \max(E_{pin})]^2 p_{in}, \quad (6)$$

where max(E_{pin}) indicates the maximum *E*-field strength

in the structure fed with a power density p_{in} and E_b=3MV/m represents the breakdown E-field strength of air. The maximum power density for the incident plane wave is thus calculated as p_{max}=(3×10^6/4926)×3.906 kW/m^2≈1.45GW/m^2.Assuming that the input power of every element is uniform, the power capacity of an element can go up to 1.45GW/m^2×0.016m^2 =371kW. However, note that this is only an estimate of the order of magnitude since in reality there are different oblique incident angles for the different elements on the reflector, and thus the input power of the different elements is non-uniform.

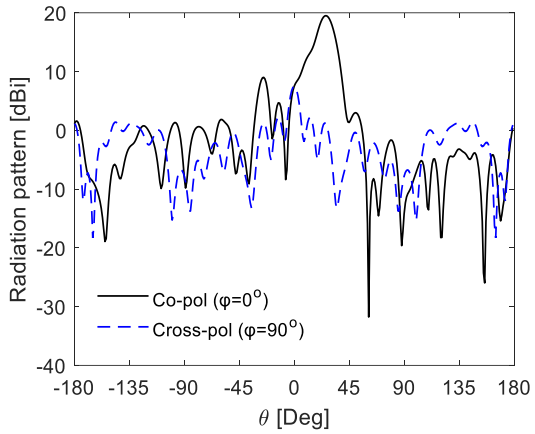

Fig. 6. Radiation pattern of the designed reflectarray at 9.3GHz: co-polar component in H plane (φ=0°) and cross-polar component in E plane (φ=90°).

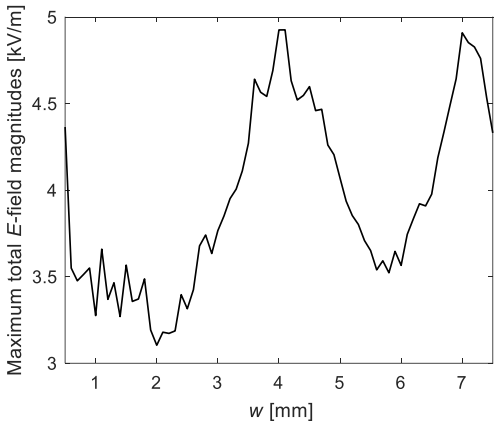

Fig. 7. Maximum total E-field magnitudes in the structure versus w.

Note that the power capacity of the structure with double square ring element covered with a polytetrafluoroethylene (PTFE) layer, as proposed in [4], is just 162kW, and the one of the structure with end-loaded dipoles, as proposed in [8], is just 150kW. The dielectric element proposed in this paper is obviously superior to the printed metallic elements for high power handling in reflectarrays as available in literature.

V. MEASUREMENTS

To verify the operational principle of our reflectarray design, a prototype of 10×10 elements was fabricated using low-cost FDM 3D printing technology. The dielectric material used is DSM's Somos® Imagine 8000 with the relative permittivity ε_r=3.4 at 1 MHz and unknown loss tangent, and a copper plate is used as ground. Figure 8 (a) shows the prototype of the reflector. The chosen feed horn was an HD-100HAT9 from HD Microwave Studio working in X-band [12]. For this horn, θ_e=38°, so that for the 10×10 array with D=160 mm the focal distance becomes F=102mm. In the actual prototype, the approximating value F=100mm was used, both in simulations and measurements. An Agilent E8257D signal generator (10MHz-40GHz) was used as source. A similar horn antenna was used as receiving antenna. The measurement set-up is shown in Fig. 8 (b).

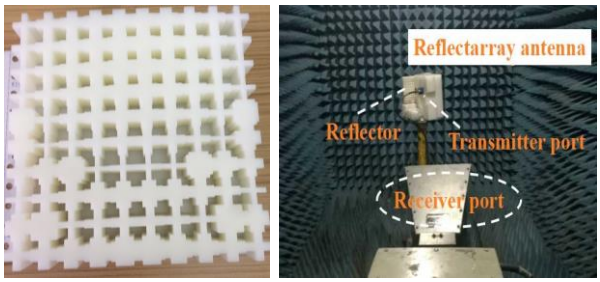

(a) (b)

Fig. 8. Photograph of the fabricated reflectarray under test in anechoic chamber. (a) Prototype of reflector, and (b) measurement set-up.

Figure 9 shows the radiation patterns at 9.3GHz, both the measured one and the ones simulated for relative permittivities ε_r=3.4 and ε_r=2.5, respectively, and an assumed loss tangent of 5.1×10^{-3} for the dielectric material. The measured gain is 15.8dBi in the direction of 20.4°. The simulated gain is 17.2dBi in the direction of 23° with ε_r=2.5, and 19.5dBi in the direction of 25° with ε_r=3.4. Comparing the measurements and simulations, the gain difference and the beam direction offset are 1.4dB and 2.6° for ε_r=2.5, while they are 3.7 dB and 4.6° for ε_r=3.4, respectively. The main reason for the observed discrepancies is the fact that the relative permittivity ε_r is actually less than 3.4 and decreases gradually with an increase of frequency. In fact, the material DSM's Somos® Imagine 8000 used in FDM 3D printing is similar as an acrylonitrile butadiene styrene (ABS) and its relative permittivity ε_r approaches 2.5 at 9.3GHz [9]. This explains the reasonable agreement between measurements and simulations with ε_r=2.5 at 9.3GHz. Second, the surface fabrication error for the reflector when using

FDM technology according to the vendor is ±0.2mm, which is larger than for traditional manufacturing techniques. This may also introduce phase compensation errors compared with the design, resulting in a beam direction shift and gain reduction.

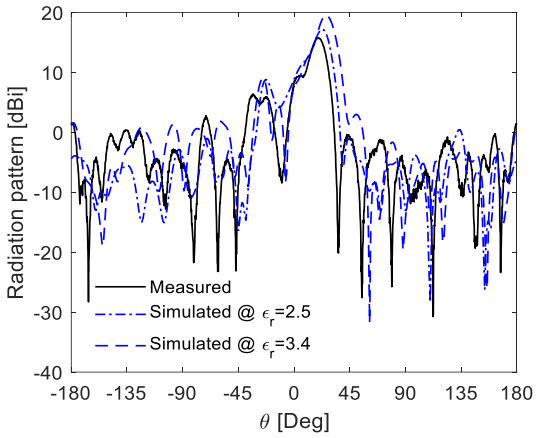

Fig. 9. Radiation pattern of the prototype reflectarray at 9.3GHz in *H* plane.

The simulated and measured gains as a function of frequency from 8.5GHz to 10GHz are given in Fig. 10. The relative permittivity ε_r=2.5 is used in the simulation. The gains increase with increasing frequency. The maximum gain difference between measurements and simulations is less than 1.4dB in this bandwidth. The proposed reflectarray satisfies the requirement of reaching a 100MHz bandwidth centered at 9.3GHz. The simulated aperture efficiency is 17.0% at 9.3GHz, 18.5% at 10GHz when ε_r=2.5, and the measured aperture efficiency is 12.3% and 16.5% at 9.3GHz and 10GHz, respectively.

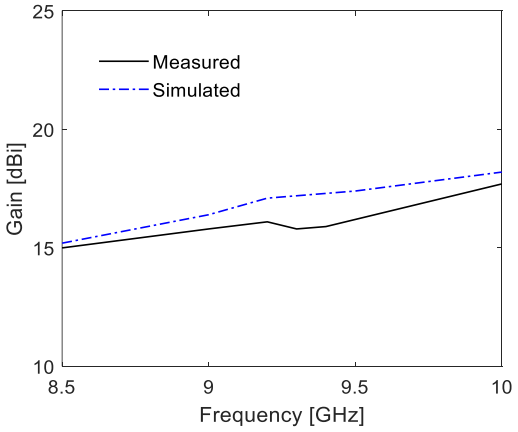

Fig. 10. Gain of dielectric reflectarray in *H* plane.

VI. CONCLUSION

A new dielectric cross-shaped reflectarray element is proposed that allows to continuously changing the effective relative permittivity in order to realize a correct reflection phase shift for reflectarray purposes. The new element provides a simple and effective method for implementing high power reflectarrays. A prototype antenna based on the element has been fabricated with 3D printing technology. A good qualitative agreement between simulated and measured results has been realized.

ACKNOWLEDGMENT

This work was supported in part by the National Natural Science Foundation of China under Grant 61471293 and the China Scholarship Council under Grant 201706285142.

REFERENCES

[1] J. Huang and J. A. Encinar, *Reflectionarray Antennas*. Hoboken-Piscataway, NJ, USA: Wiley-IEEE Press, 2007.

[2] S. H. Zainud-Deen, S. M. Gaber, A. M. Abd-Elhady, et al., "Perforated dielectric resonator antenna reflectarray," *Applied Computational Electromagnetics Society Journal*, vol. 26, no. 10, pp. 848-855, 2011.

[3] J. A. Bossard, C. P. Scarborough, Q. Wu, et al., "High-power considerations in metamaterial antennas," *Proc. IEEE Antennas Propag. Soc. Int. Symp.*, pp. 539-540, July 2014.

[4] J. Zhao, H. Li, and T. Li, "Design of a double square rings element for high-power X-band reflectarray antenna," *Proc. IEEE International Vacuum Electronics Conference*, Beijing, China, pp. 1-2, Apr. 2015.

[5] M. D. Gregory, J. D. Binion, D. Z. Zhu, et al., "High power metasurface reflectarray antennas using switched shorted circular elements," *IEEE International Symposium on Antennas and Propagation & USNC/URSI National Radio Science Meeting*, San Diego, CA, USA, pp. 1037-1038, July 2017.

[6] M. D. Gregory, J. A. Bossard, Z. C. P. O. Morgan, et al., "Metamaterials for high power reflectarray design," *IEEE/ACES International Conference on Wireless Information Technology & Systems*, Honolulu, HI, USA, pp. 1-2, Mar. 2016.

[7] M. D. Gregory, J. A. Bossard, Z. C. P. O. Morgan, et al., "A low cost and highly efficient meta-material reflector antenna," *IEEE Transactions on Antennas & Propagation*, vol. 66, no. 3, pp. 1545-1548, 2018.

[8] CST Microwave Studio, ver. 2014, Computer Simulation Technology, Framingham, MA, 2014.

[9] D. V. Isakov, Q. Lei, F. Castles, et al., "3D printed anisotropic dielectric composite with metamaterial features," *Mater. Design*, vol. 93, pp. 423-430, Mar. 2016.

[10] X. Chen, T. M. Grezegorczyk, B. I. Wu, et al., "Robust method to retrieve the constitutive effective parameters of metamaterials," *Phys. Review E*, vol. 70, no. 2, 2004.

[11] Ansoft High Frequency Structure Simulation (HFSS), ver. 15, Ansoft Corporation, Pittsburgh, PA, 2015.

[12] H. D. Wu, "HD Microwave User's Manual," 8th ed., 2017. [Online] Available: http://www.hengdamw.com/microwave-millimeterwave-antennas/standard-gain-horn-antenna.html